Computational Fluid Dynamics Model of Wells Turbine for Oscillating Water Column System: A Review

Abdul Settar, N.[1,2], Sarip, S.[1]* and Kaidi, H.M.[1]

[1] Razak Faculty of Technology and Informatics, Universiti Teknologi Malaysia, Malaysia
[2] Faculty of Engineering and Life Sciences, Universiti Selangor, Malaysia

***Corresponding author: shamsuls.kl@utm.my**

Abstract. Wells turbine is an important component in the oscillating water column (OWC) system. Thus, many researchers tend to improve the performance via experiment or computational fluid dynamics (CFD) simulation, which is cheaper. As the CFD method becomes more popular, the lack of evidence to support the parameters used during the CFD simulation becomes a big issue. This paper aims to review the CFD models applied to the Wells turbine for the OWC system. Journal papers from the past ten years were summarized in brief critique. As a summary, the FLUENT and CFX software are mostly used to simulate the Wells turbine flow problems while SST k-ω turbulence model is the widely used model. A grid independence test is essential when doing CFD simulation. In conclusion, this review paper can show the research gap for CFD simulation and can reduce the time in selecting suitable parameters when involving simulation in the Wells turbine.

1. Introduction

Ocean energy is among the primary sources of renewable energy other than Solar, Wind, Hydroelectric, Biomass, Geothermal [1]. Under ocean energy, wave energy is considered energy with a high potential as a renewable energy, but it is mainly untapped [2]. The main benefit of wave energy is having high energy density [3], high source availability [4], high load factor [3], source predictability compared to other renewable energy sources [3] and environmentally friendly [3]–[5]. A machine that absorbs wave energy and converts it into useful energy is called a wave energy converter (WEC).

The oscillating water column (OWC) is a wave energy converter (WEC) system with a simple working principle but has good efficiency. When the wave is at the crest, water will go into the water chamber and increase the water column. This water column will push and compress the air in the air chamber. The compressed air located in the air chamber then will push the blade at the air turbine, thus generating power. This is called exhalation process. Meanwhile, for the inhalation process, as the wave is at a trough, the water column will decrease, and the air will expand again. Even though the air is expanded, there will be no reverse rotation of the blade turbine, as it was designed to move only in one direction. This cycle is repeated continuously as wave crest and trough and will generate power. There are several types of turbines used in this OWC system.

The air turbine is the heart of the OWC system. Wells and Impulse turbines are the most common turbines used to compare to the cross-flow, Savonius [6], Hanna [7], or even Denniss-Auld [8] types. Although the operational flow range of the impulse turbine is wider than the Wells turbine, its peak efficiency hardly exceeds about 50 %, the main reason why the study focused more on the Wells turbine [8].

The early development of the Wells turbine created by Arthur Alan Wells in 1976 was based on the researchers' experiments, which was considered time and cost-consuming. Thus, in brief, this paper

summarises that the time taken to select appropriate parameters in doing future CFD simulations can be reduced.

2. Wells Turbine

Wave energy converter can be divided into several types as shown in Figure 1. Includes fixed structure, floating, submerged, and floating structure with concentration i.e. wave dragon. All these types of WECs described have the unique advantage of producing the same function and purpose. Figure 2 shows the typical arrangement of the OWC system with the working principle of the system [6]. Inside the air chamber contains a very important device in a WEC which is a turbine. The Wells turbine as shown in Figure 3(a) was placed at the hub which is connected to a shaft. This shaft is responsible for rotating the generator to generate the power output. The Wells turbine was placed in an enclosure casing. The turbine can only rotate in one direction regardless of the air oscillating flow direction. This is due to the symmetrical blade profile used in the Wells turbine. The symmetrical blade profile usually belongs to the NACA 00XX series.

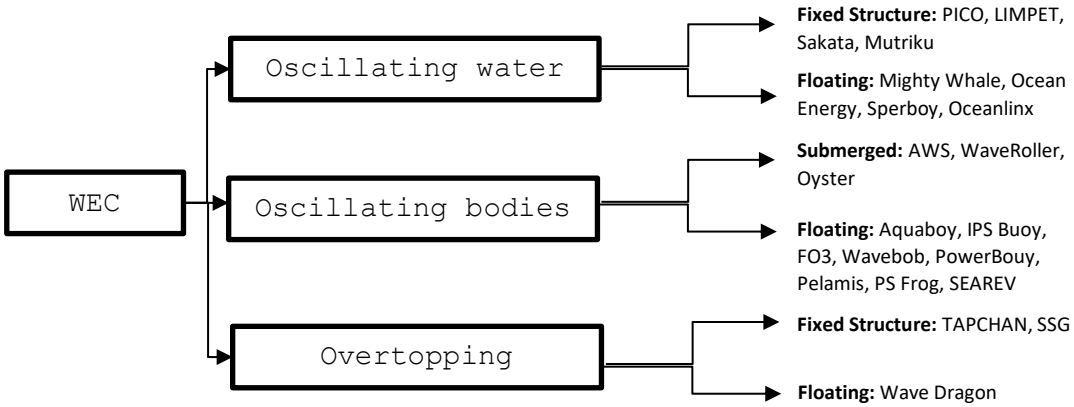

Figure 1. The various wave energy technologies [9]

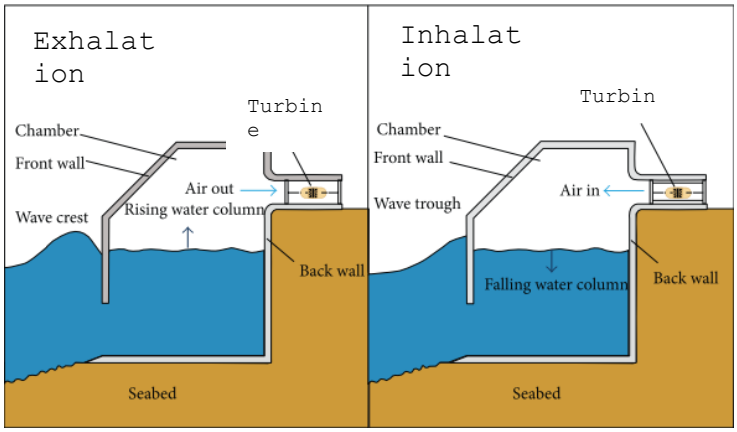

Figure 2. Typical schematic of an OWC wave energy converter [10]

Several types of Wells turbines were investigated by the researchers [8], [11]–[14]. The simplest is the single-plane Wells turbine as shown in Figure 3(a). This type of turbine just has one set of Wells turbines on one plane. The other type of Wells turbine is a biplane Wells turbine, which means that the turbine is arranged in two planes. Wells turbine with guide vanes is another type of Wells turbine as shown in Figure 3(b). The guide vanes can be placed for single plane and biplane Wells turbine. As for the biplane Wells turbine, the guide vanes can be placed in the outer or intermediate direction of the turbine. The biplane with both turbines moving in different directions is called a contra-rotating Wells turbine. The least concerned Wells turbine is the self-pitching Wells turbine, which means that the

turbine does not have a fixed pitch angle, but the angle is set free to follow the direction of the oscillating flow. The fundamental theory for each of these types was mentioned briefly by Falcão and Gato [11].

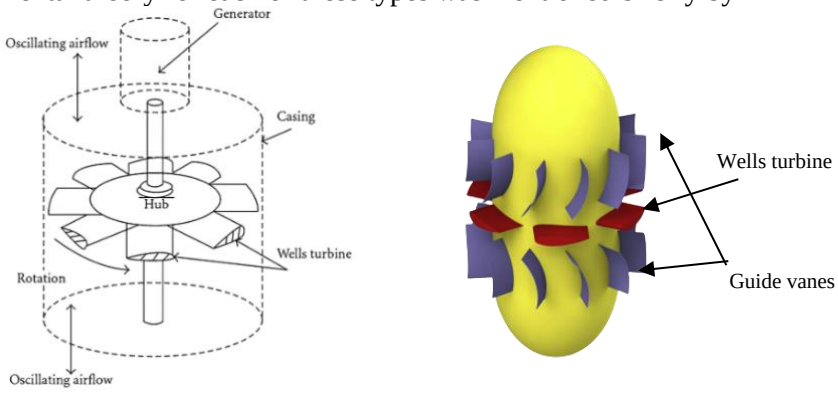

(a) (b)

Figure 3. (a) Standard single plane Wells turbine [15] and (b) single plane Wells turbine with guide vanes [16]

Optimizing the Wells turbine is focused on the blade of the Wells turbine. There are eight important parameters in optimizing the Wells turbine which are the blade profile (thickness ratio), blade solidity, blade pitch angle, blade end plate, blade aspect ratio, blade sweep, blade tip clearance and blade tip ratio [17]. According to Das, Halder, and Samad, blade solidity and tip clearance are the most important parameters among the many parameters that influence the performance of the Wells turbine [6].

The main concern of optimizing the Wells turbine is to maximize the performance of the turbine. Power output, flow rate, operational range, efficiency and pressure drop are the main parameters used as an indicator for Wells turbine performance [17]. These factors relate to each other. Thus, the most important parameter should be focused on when designing and optimizing the Wells turbine. In most cases, having a wide operating range is preferable compared to the efficiency of the turbine [6].

3.Methodology

Journals on CFD simulation on the air and hydraulic Wells turbine in the past ten years have been selected. Theses and reports were not considered in the selection. From the selected journals, the turbulence model used with the corresponding Reynolds number together with the number of elements used during the simulation are tabulated in Table 1. The mesh and type of topology used during the simulation were placed at the last column of Table 1.

4. Discussion

Before running CFD simulation in the software, important settings should be incorporated into the software. These settings are important and essential to obtain accurate and correct results. Table 1 shows the settings used in the simulation by the researchers. The table consists of the year with reference, the turbulence model used in their CFD simulation, Reynolds number obtained for the simulation, number of elements, and mesh or topology used in the simulation. A brief review on each of the setting is mentioned in the next sub-section.

Table 1. Simulation internal setting used by the researchers.

Year [Ref]	Turbulence Model	Reynolds Number	No of Elements	Mesh / Topology
2010 [18]	R k–ε	0.74×10^5, 4.41×10^5	295,500	ST, HX, OG
2011 [19]	R k–ε	0.68×10^5, 4.41×10^5	295,500	ST, HX, OG
2011 [20]	R k–ε	2.4×10^5	2,120 60,000* 80,000* 119,000	NA
2011 [21]	SST k-ω	NA	4,000,000	ST, HX, MB

Year [Ref]	Turbulence Model	Reynolds Number	No of Elements	Mesh / Topology
2012 [22]	R k–ε	NA	735,540*	ST, HX, OG, HG
			834,000	
			933,000	
			1,032,000	
			1,131,540*	
2012 [23]	R k–ε	NA	1,236,576*	ST
			1,534,016	
2012 [24]	R k–ε*, RNG k–ε, SST k-ω	NA	424,686	ST, HX
2013 [25]	R k–ε	NA	1,194,320*	ST, HX
2014 [26]	SST k-ω	5×10^5	1,800,000	ST, OG
2014 [27]	R k–ε	2.4×10^5	2,120	NA
			60,000*	
			80,000*	
			119,000	
2014 [28]	SST k-ω	4.5×10^5	1,800,000	ST, OG
2014 [29]	R k–ε*, SST k-ω, S-A	6×10^4 - 2×10^5	312,951	ST
2014 [30]	SST k-ω	NA	1,425,044	ST, HX
2015 [31]	SST k-ω	NA	1,368,000	ST, HX, MB
2015 [32]	SST k-ω	NA	764,416	ST, HX
			1,424,016*	
			1,589,250	
			1,784,000	
2016 [33]	k–ε, R k–ε*, SST k-ω, R k–ε#	2.9×10^5	410,000	HM
			500,000*	
			530,000	
2016 [34]	SST k-ω	1.3×10^5 - 3.1×10^5	1,000,000	ST, CG, HG, MB
2016 [35]	k–ε, S-A*	2.2×10^5	3,000,000	PD
2016 [36]	SST k-ω	4×10^5, 8×10^5	1,300,000	ST, HX
2017 [37]	SST k-ω	NA	1,200,000	UT
			1,600,000*	
			2,200,000	
			5,400,000	
2017 [38]	k- ε, S-A, SST k-ω, γ-Re_θ*	0.8×10^5, 1.5×10^5	1,000,000	ST, CG, HG, MB
2017 [39]	k–ε, SST k-ω*	5.2×10^5	1,200,000	UT
			1,600,000*	
			2,100,000	
2017 [40]	SST k-ω	5.2×10^5	400,000	UT
			600,000*	
			800,000	
2017 [41]	R k-ε	NA	2,580,800	UT, TX
2017 [42]	S-A	NA	1,964,000	ST, CG, HG, MB
2017 [43]	SST k-ω	1.3×10^5, 3.1×10^5	1,000,000	ST, CG, HG, MB
2017 [44]	R k-ε	NA	266,756	ST, OG, HG
			990,204	
			1,571,704*	
			1,755,876	
2017 [45]	R k-ε	NA	799,594	ST, OG, HG
			941,732	
			1,114,358	
			1,307,852	
			1,550,154*	
2018 [46]	SST k-ω	1×10^5	24,500	CG, HG
			35,000*	
			45,500	
			700,000	
			1,000,000*	

			1,300,000	
2018 [47]	R k-ε	NA	1,400,000	UT, HX
2018 [48]	R k-ε	NA	1,440,182	UT, TX
			2,113,775	
			2,580,800*	
			3,470,241	
			4,057,831	
2018 [49]	SST k-ω	5.33 x 10^5	1,045,600	ST, MB
			1,460,250*	
			1,530,200	
			1,730,500	
			1,946,000	
			2,323,453	
2018 [50]	SST k-ω	NA	90,000*	ST, CG, MB
2018 [51]	S-A	NA	2,800,000	UT
			3,500,000	
2018 [52]	SST k-ω	NA	764,416	ST
			1,424,016	
			2,646,936	
2018 [53]	SST k-ω	2 x 10^5	1,000,000	ST, HG, CG, MB
2018 [54]	SST k-ω	NA	218,000	UT, TX
			307,000*	
			481,000	
2018 [55]	SST k-ω	NA	140,000	UT
			260,000	
			340,000*	
			480,000	
2019 [56]	SST k-ω	NA	1,200,000	UT
			1,600,000*	
			2,200,000	
			5,400,000	
2019 [57]	SST k-ω	NA	1,110,000	UT, TX
			2,540,000*	
			5,770,000	
2019 [58]	SST k-ω	6.5 x 10^5 - 6.6 x 10^5	2,413,000*	UT
			4,406,000	
			10,495,000	
2020 [59]	SST k-ω	5.25 x 10^5 - 5.43 x 10^5	1,600,000	UT
			3,700,000*	
			7,000,000	
			14,100,000	

Turbulence Model: Standard k–ε (k–ε), Realizable k–ε (R k–ε), Shear stress transport k-ω (SST k-ω), Re-Normalization Group k–ε (RNG k–ε), Spalart-Allmaras (S-A), Menter transitional model (γ-Re_θ).
Mesh: Unstructured (UT), Structured (ST), Hybrid-Mesh (HM), Hexahedral (HX), Tetrahedral (TX), Polyhedral (PD). Topology: O-Grid (OG), H-Grid (HG), C-Grid (CG), Multi-Block (MB). NA – Not Available, # - nonstandard wall function, * - used in the final simulation.

4.1 Turbulence model

Selecting the suitable turbulence model for simulation is important. An unsuitable turbulence model may lead to overprediction or underprediction of the results. Based on Table 1, 15 papers used R k–ε as the turbulence model corresponding to 36 %, while about 23 papers (55 %) used SST k-ω, three papers used the S-A model and one paper used γ-Re_θ.

Using previous data from other researchers, Mohamed et al. [6] used R k–ε. The previous researcher compared k–ε, RNG k–ε, R k–ε, SST k-ω and RSM with experimental data. Čarija et al. [24] suggested that the R k–ε model is the best fit for experimental work compared to RNG k–ε and SST k-ω models. While Shehata et al. [29] concluded that R k–ε is the best model compared to SST k-ω and S-A; however,

the results between R k–ε and SST k-ω is similar, and R k–ε uses less computing time compared to SST k-ω. In this simulation, grid-independent test was not done. Cui and Hyun [33] also concluded that R k–ε is the best model compared to k–ε, SST k-ω and R k–ε with nonstandard wall function and SST k-ω giving the highest deviation from the experimental results. The author mentioned the grid-independent test, but the outcome of the simulation was not mentioned in detail.

In contrast, Ghisu et al. [34] mentioned that SST k-ω was chosen as the turbulence model based on the previous simulation) compared with several models. The researcher will use the same model for their future works [53]. Ghisu, Puddu, and Cambuli [38] suggested that γ-Re_θ is the best model compared to k- ε, S-A, and SST k-ω. They stated that this is because the Reynolds number for the simulation is under transition period and not in turbulence period.

Hu, Li, and Wei [35] compared between S-A and k–ε model. They concluded that the S-A model predicts better than the k–ε model. But it should be known that grid independence was not done in this study. Later they used this model for another research [51]. Mahboubidoust and Ramiar [42] also used S-A as the turbulence model by using the findings by Torresi et al. [60].

Most of the early simulation studies that used SST k-ω as the turbulence model stated that this model is widely used in turbomachine CFD simulations [26], [28], [30], [61], [62]. Gratton et al. [46] used the findings by Torresi et al. [63] to use SST k-ω as the turbulence model, while Nazeryan and Lakzian [49] found that simulation using SST k-ω as the turbulence model is in good agreement with the experimental data. This finding is the same with Halder, Samad, and Thévenin [39]. Das and Samad [58], [59] using SST k-ω based on research by Douvi [64] stated that this turbulence model is suitable for NACA aerofoil simulation.

In conclusion, SST k-ω is the best turbulence model for use in the Wells turbine CFD simulation, which was supported by Douvi's [51] research on NACA aerofoil and comparison data from simulation and experiment [39], [49]. S-A turbulence model is also in good agreement with simulation and experimental data. However, this model fails to predict stall point [65]. Another good model that can be used is R k–ε. This model also produces results in line with the experimental results. It should be considered that the flow of the model should exceed the critical Reynolds number so that the model can predict the result precisely [38].

4.2 Reynolds Number

Calculating Reynolds number is very crucial in CFD simulations. Knowing Reynolds number can differentiate the flow whether it is laminar, transition, or turbulent flow. Takao et al. stated that the critical Reynolds number is 4×10^5 [66]. Thus, a simulation with a Reynolds number bigger than 4×10^5 is suitable for the turbulence model. Table 1 shows that some of the researchers did not mention the value of the Reynolds number in their simulations.

Meanwhile, some researchers have flow in transition mode, but they used the turbulence model in their simulation, which may be why some of the turbulence model results differ between researchers. Ghisu et al. [38] also stated this in their research that had transition flow, and their transition model fit well with the results compared to the turbulence models. To differentiate the flow between transition and turbulence, the critical Reynolds number should be compared. But, up-to-date, only Takao et al. stated the value of critical Reynolds number [66] as 4×10^5. As Reynolds numbers is an important factor in CFD simulation, the critical Reynolds number in simulating Wells turbine is considered as one of the research gaps as no other research was done after Takao et al. [66] in 2006. This parameter is important as the newly suggested value of the critical Reynolds number can be lower or even higher than the value suggested by Takao et al. [66], which can lead to different output.

4.3 Grid Independence test

Another important test when dealing with CFD simulation is the grid independence test. This test is done to minimize the influence of grid size on the CFD simulation results [67]. As shown in Table 1, few researchers did not run the grid independence test in their research, giving some degree of ambiguity in their CFD simulation results. In the past few years, most of the researchers included the test in their

simulation. There are also some researchers [50] that included this test in their research but did not document it properly.

Even though this test is important, there is still no a standardized test method or procedure to run the test [68]. Three common methods used in this test are the grid resolution method, general Richardson extrapolation method and grid convergence index [69]. In the reviewed paper, most of the tests used were based on the grid resolution method and only Das and Samad [58] used the grid convergence index method.

4.4 Meshing and topology

As for meshing, no researcher mentioned any advantages between the structured and unstructured or otherwise, as the meshing can be used according to suitability. It should be noted that despite the unstructured mesh being able to handle complex geometries, it requires higher computational time compared to structured mesh [70]. In general, structured mesh can be considered as sufficient to handle Wells turbine blade CFD simulation. Hybrid meshing can be used to compromise the advantages and disadvantages of structured and unstructured meshing.

It is common to use structured meshing with Hexahedral and unstructured meshing with Tetrahedral. Polyhedral meshing is the least concern meshing type. Only researcher that using Star-CCM+ used this meshing. No specific advantages are known in using this meshing. As for topology, in some complex geometry or to tackle critical parts of the simulation, the multi-block should be used together with O-Grid, H-Grid, or C-Grid. This can increase the result accuracy of the main concerning region.

5. Conclusion

In summary, 42 journal papers related to CFD simulation on Wells turbine were briefly summarised. FLUENT and CFX software were recommended to be used to simulate the Wells turbine flow problem with SST k-ω turbulence model. In order to avoid discrepancies in that result, Reynolds number of the flow should be higher than the critical Reynolds number, 4×10^5. Grid independence test is a must to reduce the error in the result. There is no specific recommendation for meshing and topology, as there is no significant improvement between structed and unstructured meshing. However, the capability of the computer should be considered when dealing with unstructured mesh.

References

[1] Turkenburg W C *et al.*, 2012, Chapter 11 - Renewable Energy, in *Global Energy Assessment - Toward a Sustainable Future*, Global Energy Assessment Writing Team, Ed. (Cambridge University Press, Cambridge, UK and New York, NY, USA and the International Institute for Applied Systems Analysis, Laxenburg, Austria: Cambridge University Press), p. 761–900.
[2] Gallucci M, 2019 At Last, Wave Energy Tech Plugs Into *IEEE Spectr.* **56** p. 8–9.
[3] Melikoglu M, 2018 Current status and future of ocean energy sources: A global review *Ocean Eng.* **148**, June 2017 p. 563–573.
[4] Tedeschi E Carraro M Molinas M and Mattavelli P, 2011 Effect of control strategies and power take-off efficiency on the power capture from sea waves *IEEE Trans. Energy Convers.* **26**, 4 p. 1088–1098.
[5] Rahman M Paul N Islam S and Rashed S, 2013 Power Generation from Sea Wave : An Approach **13**, 1.
[6] Das T K Halder P and Samad A, 2017 Optimal design of air turbines for oscillating water column wave energy systems: A review *Int. J. Ocean Clim. Syst.* **8**, 1 p. 37–49.
[7] Khare V Khare C Nema S and Baredar P, 2019, Introduction of Tidal Energy, in *Tidal Energy Systems*, p. 41–114.
[8] Falcão A F O and Henriques J C C, 2016 Oscillating-water-column wave energy converters and air turbines: A review *Renew. Energy* **85** p. 1391–1424.
[9] Falcão A F d. O, 2010 Wave energy utilization: A review of the technologies *Renew. Sustain. Energy Rev.* **14**, 3 p. 899–918.

[10] Cui Y and Liu Z, 2015 Effects of Solidity Ratio on Performance of OWC Impulse Turbine *Adv. Mech. Eng.* **7**, 1 p. 1–10.
[11] Falcão A F O and Gato L M C, 2012, Air turbines, in *Comprehensive Renewable Energy*, **8**, p. 111–149.
[12] Shehata A S Xiao Q Saqr K M and Alexander D, Jan. 2017 Wells turbine for wave energy conversion: a review *Int. J. Energy Res.* **41**, 1 p. 6–38.
[13] Takao M and Setoguchi T, 2012 Air turbines for wave energy conversion *Int. J. Rotating Mach.* **2012**.
[14] Karthikeyan T Samad A and Badhurshah R, 2014 Review of air turbines for wave energy conversion *Proc. - 2013 Int. Conf. Renew. Energy Sustain. Energy, ICRESE 2013* p. 183–191.
[15] Soltanmohamadi R and Lakzian E, Aug. 2016 Improved design of Wells turbine for wave energy conversion using entropy generation *Meccanica* **51**, 8 p. 1713–1722.
[16] Cui Y Hyun B S and Kim K, 2017 Numerical study on air turbines with enhanced techniques for OWC wave energy conversion *China Ocean Eng.* **31**, 5 p. 517–527.
[17] Gareev A, 2011, Analysis of Variable Pitch Air Turbines for Oscillating Water Column (OWC) Wave Energy Converters.
[18] Taha Z Sugiyono and Sawada T, 2010 A comparison of computational and experimental results of Wells turbine performance for wave energy conversion *Appl. Ocean Res.* **32**, 1 p. 83–90.
[19] Taha Z Sugiyono Tuan Ya T M Y S and Sawada T, 2011 Numerical investigation on the performance of Wells turbine with non-uniform tip clearance for wave energy conversion *Appl. Ocean Res.* **33**, 4 p. 321–331.
[20] Mohamed M H Janiga G Pap E and Thévenin D, 2011 Multi-objective optimization of the airfoil shape of Wells turbine used for wave energy conversion *Energy* **36**, 1 p. 438–446.
[21] Torresi M Pranzo D Camporeale S M and Pascazio G, 2011 Improved Design of High Solidity Wells Turbine *9th Eur. Wave Tidal Energy Conf.* January p. 5–9.
[22] Shaaban S and Abdel Hafiz A, 2012 Effect of duct geometry on Wells turbine performance *Energy Convers. Manag.* **61** p. 51–58.
[23] Shaaban S, 2012 Insight analysis of biplane wells turbine performance *Energy Convers. Manag.* **59** p. 50–57.
[24] Čarija Z Kranjčević L Banić V and Čavrak M, 2012 Numerical analysis of wells turbine for wave power conversion *Eng. Rev.* **32**, 3 p. 141–146.
[25] Mohamed M H and Shaaban S, 2013 Optimization of blade pitch angle of an axial turbine used for wave energy conversion *Energy* **56** p. 229–239.
[26] Starzmann R and Carolus T, Jan. 2014 Effect of Blade Skew Strategies on the Operating Range and Aeroacoustic Performance of the Wells Turbine *J. Turbomach.* **136**, 1.
[27] Mohamed M H and Shaaban S, Apr. 2014 Numerical optimization of axial turbine with self-pitch-controlled blades used for wave energy conversion *Int. J. Energy Res.* **38**, 5 p. 592–601.
[28] Starzmann R and Carolus T, Feb. 2014 Model-based selection of full-scale Wells turbines for ocean wave energy conversion and prediction of their aerodynamic and acoustic performances *Proc. Inst. Mech. Eng. Part A J. Power Energy* **228**, 1 p. 2–16.
[29] Shehata A S Saqr K M Shehadeh M Xiao Q and Day A H, 2014 Entropy generation due to viscous dissipation around a wells turbine blade: A preliminary numerical study *Energy Procedia* **50** p. 808–816.
[30] Halder P and Samad A, 2014 Effect of guide vane angle on wells turbine performance *ASME 2014 Gas Turbine India Conf. GTINDIA 2014* p. 1–7.
[31] Halder P and Samad A, 2015 Casing Treatment of a Wave Energy Extracting Turbine *Aquat. Procedia* **4**, Icwrcoe p. 516–521.
[32] Halder P Samad A Kim J H and Choi Y S, 2015 High performance ocean energy harvesting turbine design-A new casing treatment scheme *Energy* **86** p. 219–231.
[33] Cui Y and Hyun B S, 2016 Numerical study on Wells turbine with penetrating blade tip

treatments for wave energy conversion *Int. J. Nav. Archit. Ocean Eng.* **8**, 5 p. 456–465.
[34] Ghisu T Puddu P and Cambuli F, 2016 Physical Explanation of the Hysteresis in Wells Turbines: A Critical Reconsideration *J. Fluids Eng. Trans. ASME* **138**, 11 p. 1–9.
[35] Hu Q Li Y and Wei F, 2016 Preliminary results of numerical simulations of a bio-mimetic wells turbine *Proc. Int. Conf. Offshore Mech. Arct. Eng. - OMAE* **6**, August.
[36] Halder P and Samad A, 2016 Optimal Wells turbine speeds at different wave conditions *Int. J. Mar. Energy* **16** p. 133–149.
[37] Halder P and Samad A, Jun. 2017 Torque and efficiency maximization for a wave energy harvesting turbine: an approach to modify multiple design variables *Int. J. Energy Res.* **41**, 7 p. 1014–1028.
[38] Ghisu T Puddu P and Cambuli F, 2017 A detailed analysis of the unsteady flow within a Wells turbine *Proc. Inst. Mech. Eng. Part A J. Power Energy* **231**, 3 p. 197–214.
[39] Halder P Samad A and Thévenin D, 2017 Improved design of a Wells turbine for higher operating range *Renew. Energy* **106** p. 122–134.
[40] Halder P Rhee S H and Samad A, 2017 Numerical optimization of wells turbine for wave energy extraction *Int. J. Nav. Archit. Ocean Eng.* **9**, 1 p. 11–24.
[41] Hamed H Nawar M and Abd El-Maksoud R, 2017 A New Operating Concept to Enhance Wells Turbine Performance *J. Eng. Sci. Mil. Technol.* **17**, 17 p. 1–14.
[42] Mahboubidoust A and Ramiar A, 2017 Investigation of DBD plasma actuator effect on the aerodynamic and thermodynamic performance of high solidity Wells turbine *Renew. Energy* **112** p. 347–364.
[43] Ghisu T Puddu P Cambuli F and Virdis I, 2017 On the Hysteretic Behaviour of Wells Turbines *Energy Procedia* **126** p. 706–713.
[44] Shaaban S, Oct. 2017 Wells turbine blade profile optimization for better wave energy capture *Int. J. Energy Res.* **41**, 12 p. 1767–1780.
[45] Shaaban S, Mar. 2017 Wave energy harvesting using a novel turbine rotor geometry *Int. J. Energy Res.* **41**, 4 p. 540–552.
[46] Gratton T Ghisu T Parks G Cambuli F and Puddu P, 2018 Optimization of blade profiles for the Wells turbine *Ocean Eng.* **169**, July p. 202–214.
[47] González C M Fuertes G R Díaz M G García B P Castro F and Oro J M F, 2018 Wells turbine with variable blade profile for wave energy conversion *Proc. Int. Conf. Offshore Mech. Arct. Eng. - OMAE* **10** p. 1–7.
[48] Hashem I Abdel Hameed H S and Mohamed M H, 2018 An axial turbine in an innovative oscillating water column (OWC) device for sea-wave energy conversion *Ocean Eng.* **164**, June p. 536–562.
[49] Nazeryan M and Lakzian E, 2018 Detailed entropy generation analysis of a Wells turbine using the variation of the blade thickness *Energy* **143** p. 385–405.
[50] Licheri F Climan A Puddu P Cambuli F and Ghisu T, 2018 Numerical Study of a Wells Turbine with Variable Pitch Rotor Blades *Energy Procedia* **148** p. 511–518.
[51] Hu Q and Li Y, 2018 Unsteady RANS simulations of wells turbine under transient flow conditions *J. Offshore Mech. Arct. Eng.* **140**, 1 p. 1–11.
[52] Halder P Mohamed M H and Samad A, 2018 Wave energy conversion: Design and shape optimization *Ocean Eng.* **150**, September 2016 p. 337–351.
[53] Ghisu T Cambuli F Puddu P Mandas N Seshadri P and Parks G T, 2018 Numerical evaluation of entropy generation in isolated airfoils and Wells turbines *Meccanica* **53**, 14 p. 3437–3456.
[54] Kumar P M Halder P and Samad A, 2018 Performance analysis of wells turbine with radiused blade tip *Proc. Int. Conf. Offshore Mech. Arct. Eng. - OMAE* **10** p. 1–10.
[55] Madhan Kumar P Halder P Samad A and Rhee S H, 2018 Wave energy harvesting turbine: Effect of hub-to-tip profile modification *Int. J. Fluid Mach. Syst.* **11**, 1 p. 55–62.
[56] Halder P Das T K Samad A and Mohamed M H, 2019, Hysteresis Behavior for Wave Energy Conversion Device Under Alternative Axial Flow Conditions, in *Proceedings of the Fourth International Conference on Substorms*, **23**, (Springer Singapore), p. 717–723.
[57] Kumar P M and Samad A, 2019 Introducing Gurney flap to Wells turbine blade and

performance analysis with OpenFOAM *Ocean Eng.* **187**, May p. 106212.
[58] Das T K and Samad A, 2019 The effect of midplane guide vanes in a biplane wells turbine *J. Fluids Eng. Trans. ASME* **141**, 5 p. 1–13.
[59] Das T K and Samad A, 2020 Influence of stall fences on the performance of Wells turbine *Energy* **194** p. 116864.
[60] Torresi M Camporeale S M Strippoli P D and Pascazio G, 2008 Accurate numerical simulation of a high solidity Wells turbine *Renew. Energy* **33**, 4 p. 735–747.
[61] Ahmed N and Mueller M, 2013 Impact of varying clearances for the Wells turbine on heat transfer from electrical generators in oscillating water columns *2013 8th Int. Conf. Exhib. Ecol. Veh. Renew. Energies, EVER 2013* p. 3–8.
[62] Premkumar T M Ashish M A Banu Prakash T and Thulasiram D, 2014 Numerical analysis of wells turbine *Appl. Mech. Mater.* **592**–**594** p. 1125–1129.
[63] Torresi M Camporeale S M and Pascazio G, 2009 Detailed CFD analysis of the steady flow in a wells turbine under incipient and deep stall conditions *J. Fluids Eng. Trans. ASME* **131**, 7 p. 0711031–07110317.
[64] Douvi C. Eleni, Mar. 2012 Evaluation of the turbulence models for the simulation of the flow over a National Advisory Committee for Aeronautics (NACA) 0012 airfoil *J. Mech. Eng. Res.* **4**, 3.
[65] Cui Y Liu Z Zhang X and Xu C, 2019 Review of CFD studies on axial-flow self-rectifying turbines for OWC wave energy conversion *Ocean Eng.* **175**, December 2018 p. 80–102.
[66] Takao M Thakker A Abdulhadi R and Setoguchi T, 2006 Effect of blade profile on the performance of a large-scale Wells turbine for wave-energy conversion *Int. J. Sustain. Energy* **25**, 1 p. 53–61.
[67] Roychowdhury D G, 2020 *Computational Fluid Dynamics for Incompressible Flows* .
[68] Lee M Park G Park C and Kim C, 2020 Improvement of Grid Independence Test for Computational Fluid Dynamics Model of Building Based on Grid Resolution *Adv. Civ. Eng.* **2020**.
[69] Seeni A Rajendran P and Mamat H, 2019 A CFD mesh independent solution technique for low reynolds number propeller *CFD Lett.* **11**, 10 p. 15–30.
[70] Tu J Yeoh G-H and Liu C, 2013, Practical Guidelines for CFD Simulation and Analysis, in *Computational Fluid Dynamics*, (Elsevier), p. 219–273.

Acknowledgement
The authors would like to thank the Universiti Teknologi Malaysia under the Industry-International Incentive Grant scheme (Q.K130000.3601.03M09) for supporting this research.